

Steric Control over Arene Coordination to β -Diiminate Rhodium(I) Fragments

Peter H. M. Budzelaar,* Nicolle N. P. Moonen, René de Gelder, Jan M. M. Smits, and Anton W. Gal^[a]

Abstract: The bulky ligands L_x^- ($L_x = (2,6-C_6H_3X_2)NC(Me)CHC(Me)N(2,6-C_6H_3X_2)$, $X = Cl, Me$) can be used to generate fluxional mononuclear arene complexes $[L_xRh(\eta^4\text{-arene})]$ (arene = benzene, toluene, *m*-xylene, mesitylene), which for $X = Me$ disproportionate to fluxional dinuclear complexes $[[L_{Me}Rh]_2(\textit{anti-}\mu\text{-arene})]$. For both mononuclear and dinuclear complexes, steric interactions do not stop the fluxionality but govern the preferred orientation of

the methyl-substituted arenes, thus allowing indirect determination of the static NMR parameters. For the μ -arene complexes, two distinct types of fluxionality are proposed on the basis of calculations: ring rotation and metal shift. In the solid state, the toluene

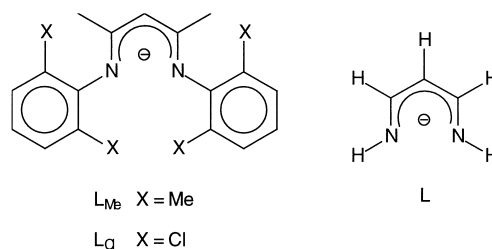
complex has an $\eta^4(1,2,3,4):\eta^4(3,4,5,6)$ -bridged structure; the NMR analysis indicates that the benzene and *m*-xylene complexes have similar structures. The mesitylene complex, however, has an unprecedented $\eta^3(1,2,3):\eta^3(3,4,5)$ -bridged structure, which is proposed to correspond to the transition state for arene rotation in the other cases. Steric factors are thought to be responsible for this reversal of stabilities.

Keywords: arene complexes • bridging ligands • density functional calculations • fluxionality • rhodium

Introduction

Arenes display an amazing variety of coordination modes to transition metals. For mononuclear systems, the η^6 arrangement is by far the most common one, but lower hapticities (η^2 , η^3 , η^4) are also frequently observed. In addition, a wide range of bridging modes are known, with the metals on the same or on opposite sides of the ring plane; triply bridging arrangements have also been reported.^[1] Following the seminal paper by Hoffmann,^[2] bonding in such complexes is usually discussed in terms of electronic preferences. Consideration of the number of valence electrons has been found useful in rationalizing the hapticities of mono- and dinuclear complexes. In contrast, the role of steric factors in determining bonding mode and orientation of the arene has received much less attention.

We recently reported how bulky β -diiminate ligands L_x^- ($X = Me, Cl$) could be used to stabilize coordinatively unsaturated olefin complexes $[L_xRh(\text{cyclooctene})]$.^[3] The



stabilization was attributed to steric shielding of the metal atom by the vertical aryl “walls” of the diiminate ligand. In the present work, we describe the formation of mono- and dinuclear arene complexes from the olefin complexes. X-ray structure determinations of the bridged arene complexes produced one example of the rare *anti*- $\eta^4(1,2,3,4):\eta^4(3,4,5,6)$ mode, and one example of the unprecedented *anti*- $\eta^3(1,2,3):\eta^3(3,4,5)$ mode. Steric factors are thought to play a crucial role here, in determining both the arene orientation and—for the dinuclear systems—the bridging mode. The intrinsic structural preferences of the system were probed by calculations for the model ligand L, to clarify the nature of these steric factors. Since the only other example of the *anti*- $\eta^4(1,2,3,4):\eta^4(3,4,5,6)$ bridging mode is a cyclopentadienyl–

[a] Dr. P. H. M. Budzelaar, N. N. P. Moonen, Dr. R. de Gelder, J. M. M. Smits, Prof. Dr. A. W. Gal
Department of Inorganic Chemistry
University of Nijmegen
Toernooiveld 1, 6525 ED Nijmegen (The Netherlands)
Fax: (+31)24-3553450
E-mail: budz@sci.kun.nl

Supporting information (ORTEP plots of the disordered cyclohexane molecules of $[[L_{Me}Rh]_2(\text{toluene})] \cdot 3C_6H_{12}$, calculated total energies for the model Co, Rh, and Ir complexes mentioned in the text, and the least squares equations used to extract the NMR parameters in Table 2) for this article is available on the WWW under <http://www.wiley-vch.de/home/chemistry/> or from the author.

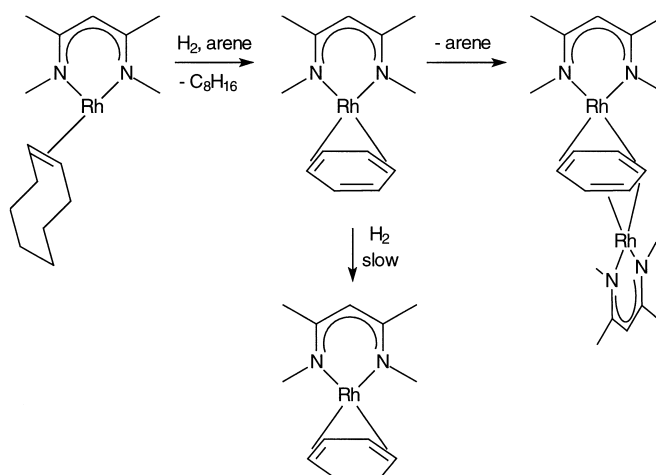
cobalt complex,^[4] the analogous cyclopentadienyl systems were included in the theoretical study.

Results and Discussion

Generation of mononuclear and dinuclear arene complexes: Mononuclear (β -diiminate)rhodium(i) arene complexes are conveniently prepared: $[\text{L}_{\text{Me}}\text{Rh}(\text{cyclooctene})]^{[\text{b}]}$ is dissolved in the arene (benzene, toluene, *m*-xylene or mesitylene), the solution is stirred under hydrogen for 30 s, and the volatiles are removed in vacuo (Scheme 1). The resulting complexes must be kept below -30°C . At room temperature in THF, disproportionation of $\text{L}_{\text{Me}}\text{Rh}(\text{arene})$ to the free arene and the μ -arene complex (see below) is complete in about 10 min. Under the same conditions, the analogous $[\text{L}_{\text{Cl}}\text{Rh}(\text{benzene})]$ complex decomposes to insoluble materials, probably by C–Cl oxidative addition.^[5] Unfortunately, we could not purify the mononuclear arene complexes by crystallization, so characterization is by NMR spectroscopy only. NMR spectroscopic data are collected in Table 1; interpretation of these data is discussed in the next section.

If the solution of $[\text{L}_x\text{Rh}(\text{cyclooctene})]$ in benzene is stirred under hydrogen for one day, formation of a cyclohexadiene complex is observed. $[\text{L}_{\text{Me}}\text{Rh}(\eta^4\text{-C}_6\text{H}_8)]$ is always contaminated with the μ -arene complex, so characterization was by NMR only. The corresponding $[\text{L}_{\text{Cl}}\text{Rh}(\eta^4\text{-C}_6\text{H}_8)]$ complex could be crystallized and its X-ray structure is given in Figure 1. The molecule has approximate C_s symmetry; the Rh coordination geometry is square planar, as expected.

As mentioned above, the mononuclear complexes $[\text{L}_{\text{Me}}\text{Rh}(\text{arene})]$ all disproportion-



Scheme 1. Preparation of mononuclear and dinuclear arene complexes.

tionate in THF at room temperature to complexes of the composition $[\{\text{L}_{\text{Me}}\text{Rh}\}_2(\text{arene})]$. The same dinuclear species are also obtained from the direct reaction of $[\text{L}_{\text{Me}}\text{Rh}(\text{cyclooctene})]$

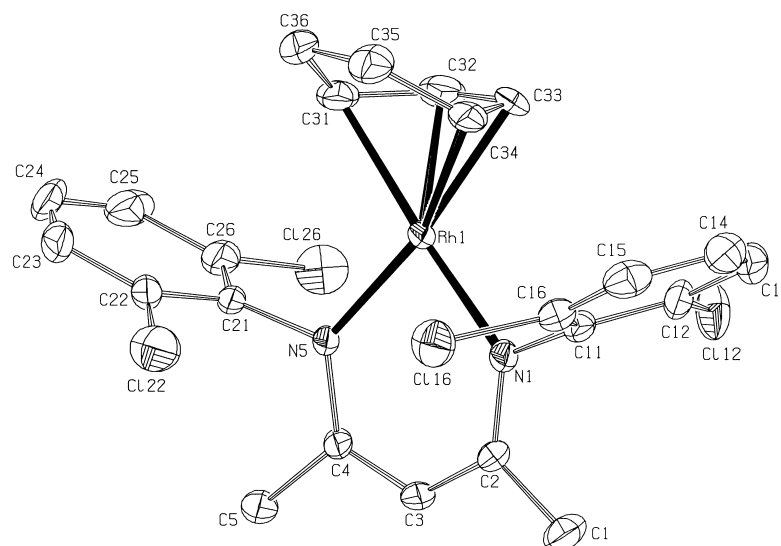


Figure 1. X-ray structure of $[\text{L}_{\text{Cl}}\text{Rh}(\text{cyclohexadiene})]$ (all hydrogen atoms have been omitted). Selected bond lengths [\AA]: C31–C32 1.397(9), C32–C33 1.434(10), C33–C34 1.366(10), C34–C35 1.498(9), C35–C36 1.501(9), C36–C31 1.495(9), Rh1–C31 2.191(6), Rh1–C32 2.092(6), Rh1–C33 2.100(5), Rh1–C34 2.152(5), Rh1 \cdots C35 2.947(6), Rh1 \cdots C36 2.992(6).

Table 1. Observed and predicted^[a] averaged shifts for $\text{L}_{\text{Me}}\text{Rh} \eta^4$ -arene and μ - η^4 : η^4 -arene complexes.

Arene	Correction ^[b]	η^4 -arene				μ - η^4 : η^4 -arene					
		^1H		^{13}C		^1H		^{13}C			
		obs	calcd	obs	calcd	obs	calcd	obs	calcd		
C_6H_6	–	–	4.49	4.41	96.5	96.8	2.12	2.14	65.6	66.7	
$\text{C}_6\text{H}_5\text{Me}$	<i>i</i>	–	–	–	–	138.4	137.5	–	–	88.4	87.0
	<i>o</i>	–0.19	+1.0	3.36	3.42	99.4	101.6	0.61	1.03	63.2	62.3
	<i>m</i>	–0.11	+0.5	4.00	3.85	82.2	81.7	1.31	1.11	59.9	61.8
	<i>p</i>	–0.17	–1.4	5.65	5.86	85.8	87.6	4.25	3.81	72.2	76.1
1,3- $\text{C}_6\text{H}_4\text{Me}_2$	1/3	–	+9.7	–	–	122.5	118.2	–	–	89.1	82.7
	2	–0.35	+2.0	1.24	1.55	76.0	75.3	0.12	–0.15	67.3	70.5
	4/6	–0.36	–1.8	5.22	5.31	104.2	106.7	2.35	2.75	62.3	64.0
	5	–0.19	+0.2	1.79	1.71	75.0	73.5	2.72	2.43	59.0	54.3
1,3,5- $\text{C}_6\text{H}_3\text{Me}_3$ ^[c]	1/3/5	–	+9.6	–	–	106.3	106.4	–	–	103.1	76.3
	2/4/6	–0.61	–0.6	3.71	3.80	96.1	96.2	0.90	1.53	58.1	66.1

[a] Using the “intrinsic” shifts from Table 2. [b] Shift of position in free arene relative to free benzene. [c] Not included in fit.

tene)] with arene, but this reaction is much slower at room temperature (several days in pure arene). The X-ray structure of the toluene complex (Figure 2) shows an arene ring bridging between two metal atoms in an *anti-μ-η*⁴(1,2,3,4):*η*⁴(3,4,5,6) fashion. The arene ring has one long, localized

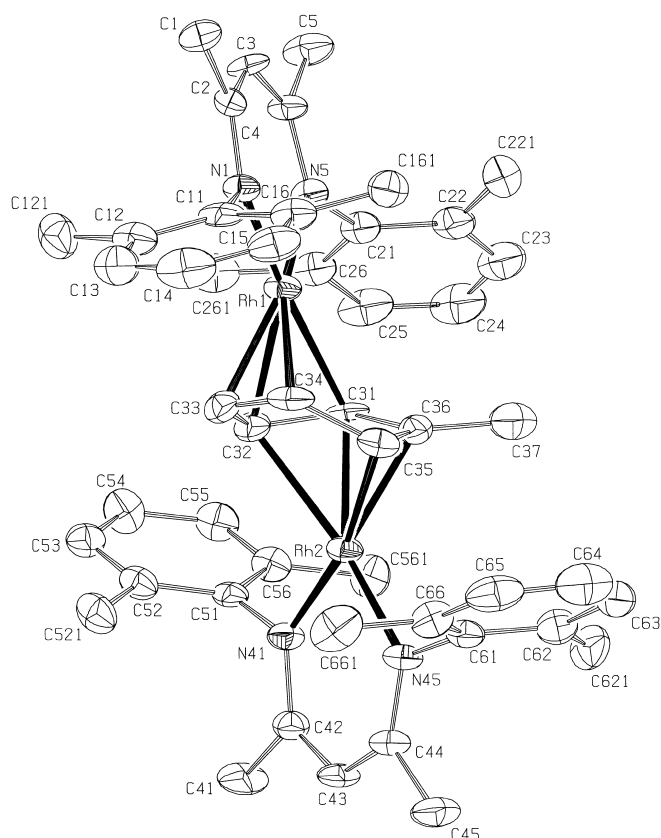


Figure 2. X-ray structure of $[[L_{Me}Rh]_2(\text{toluene})]$ (the three molecules of cyclohexane of crystallization and all hydrogen atoms have been omitted). Selected bond lengths [Å]: C31–C32 1.447(13), C32–C33 1.433(13), C33–C34 1.379(14), C34–C35 1.484(15), C35–C36 1.410(13), C36–C31 1.438(13), Rh1–C31 2.328(9), Rh1–C32 2.237(9), Rh1–C33 2.051(10), Rh1–C34 2.212(10), Rh1...C35 2.943(11), Rh1...C36 2.875(9), Rh2–C35 2.199(10), Rh2–C36 2.069(9), Rh2–C31 2.188(8), Rh2–C32 2.330(10), Rh2...C33 2.897(10), Rh2...C34 2.945(9); angle between Rh–Rh vector and arene least-squares plane is 85.5°.

single bond (C31–C36) and is decidedly nonplanar. Each Rh atom is bound to one formal double bond; in addition, the two Rh atoms share the remaining double bond. Each Rh–“diene” interaction is similar to that in the cyclohexadiene complex described above. Judging from the Rh–C distances, interactions with the shared double bond are somewhat weaker than with the nonshared bonds. There is only one literature report of this kind of arene bridging: the structure of $[[Cp^*Co]_2(\text{cumene})]$ also has a *η*⁴(1,2,3,4):*η*⁴(3,4,5,6) structure, with a very similar pattern of bond lengths.^[4]

The physical properties of the dinuclear benzene, toluene, and *m*-xylene complexes are rather similar, but the mesitylene complex shows a much lower solubility in organic solvents (alkanes, THF), suggesting a different structure. The X-ray structure (Figure 3) shows an unprecedented *anti-μ-η*³(1,2,3):*η*³(3,4,5) structure in which the Rh atoms share one carbon

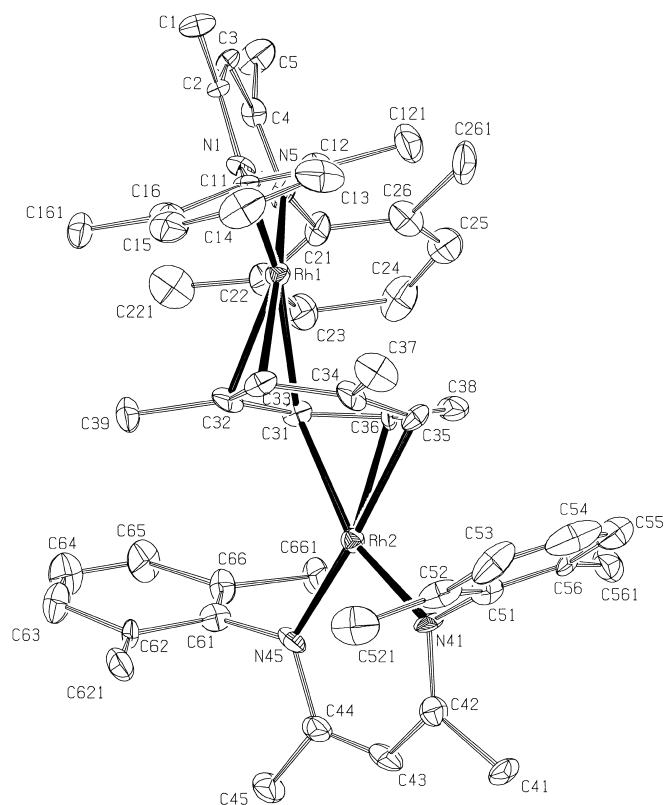


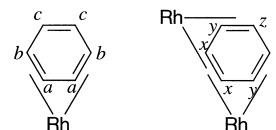
Figure 3. X-ray structure of $[[L_{Me}Rh]_2(\text{mesitylene})]$ (all hydrogen atoms have been omitted). Selected bond lengths [Å]: C31–C32 1.45(2), C32–C33 1.417(16), C33–C34 1.42(2), C34–C35 1.38(2), C35–C36 1.421(16), C36–C31 1.430(18), Rh1–C31 2.326(19), Rh1–C32 2.050(10), Rh1–C33 2.148(11), Rh1...C34 2.698(16), Rh2–C31 2.342(19), Rh2–C36 2.084(11), Rh2–C35 2.194(12), Rh2...C34 2.747(15); angle between Rh–Rh vector and arene least-squares plane is 83.1°.

atom (C31), while the arene carbon atom *para* to it (C34) is not directly bonded to a metal atom. In this case, the arene ring is approximately planar. The significance of this and alternative bridging modes will be discussed in more detail later on.

NMR data of *η*⁴-arene complexes: The NMR spectra of mononuclear $[L_xRh(\text{arene})]$ complexes indicate a high apparent symmetry. This can be explained either by an *η*⁶-bound structure or by a highly fluxional structure of lower hapticity. However, an *η*⁶ bonding mode is rather unlikely, since that would be expected to give rather similar shifts for all carbons of the toluene and *m*-xylene ligands, whereas the observed spread in shifts (see Table 1) is very large (75 to 104 ppm). In fact, we find that the NMR data can be analyzed satisfactorily in terms of an *η*⁴ model.^[6]

The analysis requires two assumptions:

1) Independent of the methyl substitution pattern, an arene carbon can occupy one of three distinct “sites” (*a*, *b*, *c*), each with a different “intrinsic chemical shift”. The observed shift(s) will be time-averages over the different sites.



2) The methyl substitution pattern of the ring will induce a dominant preferred orientation of the ring relative to the $L_{Me}Rh$ fragment. This seems reasonable because the methyl groups are expected to avoid the ligand “walls”. There will always be several equivalent orientations, so the observed shifts are still averages, but the shifts will be averaged in different ways for different methyl substitution patterns.

Methyl substitution also directly affects the chemical shifts of the ring protons and carbons; this can be approximated by the analogous effect in the free arene. If the data obtained for benzene, toluene and *m*-xylene are combined, an overdetermined system of equations is obtained which can be solved by linear least squares. The resulting intrinsic shifts are collected in Table 2, and the time-averaged shifts predicted from these intrinsic shifts are compared with the observed values in Table 1. The agreement is seen to be quite good, with an average deviation of 0.15 ppm for 1H and 1.5 ppm for ^{13}C . The agreement for mesitylene, which was not included in the fit, is equally good. Of the three intrinsic ^{13}C shifts, one (*c*, 128 ppm) is typical for a free olefin or arene. The other two show strong high-field shifts typical for coordination to a metal, similar to those observed for the cyclohexadiene complex (included in Table 2 for comparison). Thus, these data clearly support an η^4 structure.^[6] In the toluene complex, the methyl group is in position *c*, that is, it avoids the metal-bound arene positions.

Interpretation of the intrinsic 1H shifts is less straightforward, since these will be affected not only by coordination to the metal but also by the anisotropy of the diiminate aryl substituents. For position *b*, where both effects work in the same direction, we obtain an extremely high-field shift of 1.90 ppm. The intrinsic 1H shifts for positions *a* and *c* are rather similar, and we cannot conclude from the 1H parameters alone which of the two belongs to the Rh-bound part of the ring. However, the ^{13}C parameters are unambiguous in this respect, and we find that—curiously—the 6.03 ppm value corresponds to the coordinated part of the ring.

NMR data of μ -arene complexes: The NMR spectra of the dinuclear species $[(L_{Me}Rh)_2(arene)]$ also indicate a high degree of fluxionality. Again, the toluene and *m*-xylene complexes show effective C_{2v} symmetry, indicating that, relative to the X-ray structure of Figure 2, both double-bond shift and movement of the Rh atoms over the ring must be fast. Therefore, the NMR parameters will again be time-averages over different sites (*x*, *y*, *z*), which can be analyzed as

described for the mononuclear complexes. This time, the agreement between predicted and observed shifts is poorer, and the standard deviations in the intrinsic NMR parameters are twice as large. It may be that the methyl substituents cause larger structural distortions in these dinuclear complexes, making the assumption of constant intrinsic shifts less justified. The very large discrepancies in the calculated shifts for the μ -mesitylene complex, which was not included in the fit, suggest that it has a different type of structure, which is confirmed by X-ray diffraction.

In principle, the assignments for *x* and *z* could be exchanged (but only for 1H and ^{13}C simultaneously). However, it is possible to estimate the intrinsic shifts for the dinuclear complexes from those of the mononuclear ones. Position *y* should experience the coordination shift Δa of position *a* plus the nonbonded shift Δc of position *c*; similarly position *z* should feel $\Delta b + \Delta c$. The shared double-bond position *x*, which is more weakly bound than the other double bonds, should experience some fraction φ of $\Delta a + \Delta b$. Table 2 shows that a reasonable agreement for both 1H and ^{13}C NMR data is obtained when φ is taken to be 0.75; a similar agreement between the shifts for *a* to *c* and *x* to *z* cannot be obtained when the assignments for *x* and *z* are reversed. This supports the assignment given in Table 2.

The toluene methyl group is in position *y* because this is the only way to avoid repulsion with *both* ligand walls. In the *m*-xylene complex, the first methyl group also occupies this position; the second methyl group must always point towards a wall of one $L_{Me}Rh$ fragment. With the above assignment, it takes position *z*, which is bound to only one Rh atom, and thus avoids shared position *x*.

The value of φ gives an indication of the effectiveness of donation from the “shared” double bond. A value of 0.5 would mean that in the bridged complex each metal atom would get only half of the interaction it gets in the mononuclear complex; a value of 1.0 would mean that each metal gets as much from the bond as it would get if the other metal was not present. The intermediate value of 0.75 indicates that donation to one metal reduces the donor capacity of the double bond for further donation, but does not completely suppress it.

Structure of mononuclear arene complexes: The η^4 structure of the mononuclear arene complexes proposed on the basis of the NMR data might at first sight seem peculiar, since these

Table 2. Intrinsic NMR parameters for $L_{Me}Rh \eta^4$ -arene and μ - η^4 : η^4 -arene complexes.^[a]

Observed ^[b]			From fit			From fit			Predicted ^[c]	
site	1H	^{13}C	site	1H	^{13}C	site	1H	^{13}C	1H	^{13}C
<i>a</i>	4.26	79.5	<i>a</i>	6.03(12)	89.0(15)	<i>x</i>	2.24(32)	54.0(23)	2.32	57.7
<i>b</i>	1.64	72.4	<i>b</i>	1.90(10)	73.3(15)	<i>y</i>	3.98(28)	77.5(23)	4.08	89.0
			<i>c</i>	5.32(17)	128.0(15)	<i>z</i>	0.20(32)	68.5(23)	−0.05	73.3

[a] All values in ppm. Estimated standard deviations (1σ , from fit) in parentheses. [b] Included for comparison only. [c] Calculated from the parameters for the mononuclear complex (see text), with $\varphi = 0.75$.

are only 16e structures. To clarify this point, we have carried out B3LYP calculations on the model system [LRh(benzene)]. These confirm the preference for non- η^6 structures. The preference is not very large, and movement of the LRh fragment over the ring is nearly free, but the lowest-energy structures were found to be η^4 and η^2 . The NMR analysis is not compatible with an η^2 structure for the “real” complexes. The η^2 structure may still be involved in the fluxional behaviour of these complexes, but in view of the easy movement of LRh over the ring it might not be meaningful to speak of distinct “mechanisms” for fluxionality here.

The preference for a 16e η^4 structure may be rationalized as follows. In principle, the LRh fragment has three empty valence orbitals. The two lying in the plane of the diiminate ligand are low in energy and are used for normal 16e square-planar [LRh(donor)₂] complexes; these are enough to form an η^4 -arene complex. The third acceptor orbital is mostly p_z in character. It is much higher in energy than the other two and has a poor overlap with the relevant arene π -orbital. The use of this orbital to form an η^6 structure can apparently not compensate for the resulting repulsion with filled Rh 4d orbitals. Replacement of the σ -donating diiminate ligand by stronger π -acceptor ligands like phosphanes lowers the third acceptor orbital, resulting in 18e η^6 structures.^[2, 7]

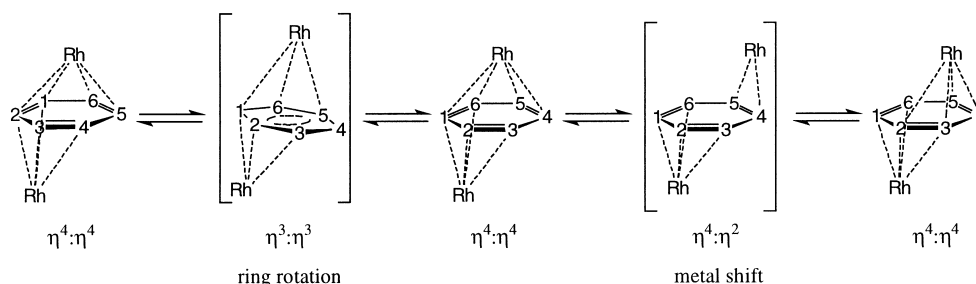
Structure and fluxionality of anti-bridged dinuclear arene complexes: For the *anti*-bridged dinuclear arene complexes we again used calculations to clarify the bonding situation. Regardless of the orientation of the arene ring between the two metal atoms, all low-energy structures have nearly orthogonal diiminate planes. If only the two in-plane acceptor orbitals of each LRh fragment are considered, this means that they compete for the lowest (symmetric) arene π -orbital, but that each interacts with a *different* arene π -HOMO; in a parallel orientation they would also compete for the same π -HOMO while leaving the other one unused.

Calculations for the model system [(LRh)₂(benzene)] revealed three low-lying stationary points (Scheme 2): an $\eta^4(1,2,3,4):\eta^2(5,6)$ structure, an $\eta^4(1,2,3,4):\eta^4(3,4,5,6)$ structure and an $\eta^3(1,2,3):\eta^3(3,4,5)$ structure, all within 6 kcal mol⁻¹ of each other.^[8] They are connected by two paths, one corresponding to movement of one LRh fragment over the benzene ring (“metal shift”) and the other to in-place rotation of benzene with nearly stationary LRh fragments (“ring rotation”). In the calculations, the $\eta^4:\eta^2$ structure is slightly lower in energy than the $\eta^4:\eta^4$ one; the X-ray structure of [(L_{Me}Rh)₂(toluene)] and the NMR data for the analogous

benzene and *m*-xylene complexes show that in these “real” L_{Me} systems the $\eta^4:\eta^4$ structure is preferred. The pattern of bond lengths calculated for the $\eta^4:\eta^4$ -[(LRh)₂(benzene)] complex agrees with the X-ray structure of the [(L_{Me}Rh)₂(toluene)] complex.^[9] If we assume that the two low-energy rearrangements calculated for the benzene model system are the only ones possible in solution for all arene complexes, then *both* must be occurring: arene rotation alone would not result in C_{2v} symmetry of the ligands, and metal shift alone would not exchange the “single” and “double” bonds of the $\eta^4:\eta^4$ structure.

Methyl substituents on the arene will try to avoid the ligand “walls”. For the mesitylene complex in an $\eta^4:\eta^4$ structure, two methyl groups will always point towards a wall. We believe that this is the reason the mesitylene complex prefers the observed $\eta^3:\eta^3$ structure, which would otherwise be the transition state for arene rotation. Given that the calculated energy difference between $\eta^4:\eta^4$ and $\eta^3:\eta^3$ structures is only 6 kcal mol⁻¹ for the model compound, such a reversal of stabilities by steric effects does not appear unreasonable. Again, the pattern of calculated distances for this structure is similar to that found in the X-ray structure determination.^[9]

syn- versus anti-bridged structures: There is only one earlier report of the *anti*- $\eta^4(1,2,3,4):\eta^4(3,4,5,6)$ arene bridging mode described here, namely the cobalt complex [(Cp*Co)₂(cumene)].^[4] Remarkably, the rhodium complexes [(CpRh)₂(benzene)]^[10] and [MeSi{C₅H₄Rh(C₂H₄)₂}{C₅H₄Rh}₂(benzene)]^[11] prefer a *syn-μ*- $\eta^3(1,2,3):\eta^3(4,5,6)$ structure with a metal–metal bond, as do the isoelectronic complexes [(η^6 -toluene)Fe]₂(toluene)]^[12] and [(CO)₃Ru]₂([2.2]paracyclophane)].^[13] This raises the question whether the preference for *syn* or *anti* bridging is influenced by the metal (Co/Rh), by the ligand (cyclopentadienyl versus diiminate), or both. To answer this question, we decided to systematically compare the diiminate and cyclopentadienyl derivatives of the three metals Co, Rh and Ir.^[14] Despite the differences in formal electron count of the LM (12e) and CpM (14e) fragments, the calculated structures are rather similar. Mononuclear Cp and diiminate complexes uniformly prefer η^4 structures. Dinuclear complexes *always* prefer the *syn-μ*- $\eta^3(1,2,3):\eta^3(4,5,6)$ structure observed for [(CpRh)₂(benzene)] (see Table 3). For [(Cp*Co)₂(cumene)] and our β -diiminate complexes, however, *syn* bridging is not possible for steric reasons, and the *anti*-bridged structure results as a “second-best”. All complexes show relatively easy arene rotation; the highest barriers were found for Ir, as shown in Table 4.



Scheme 2. Low-energy structures of dinuclear arene complexes and the paths connecting them.

Table 3. Calculated relative stabilities of *syn*- and *anti*-bridged arene complexes [kcal mol⁻¹].

Complex	Co	Rh	Ir
[[LM] ₂ (C ₆ H ₆)] <i>anti</i> above <i>syn</i>	8.3	13.1	16.4
[[CpM] ₂ (C ₆ H ₆)] <i>anti</i> above <i>syn</i>	14.0	18.2	33.5

Table 4. Calculated barriers for fluxional processes in μ -arene complexes [kcal mol⁻¹].

Complex	Process	Co	Rh	Ir
[[CpM] ₂ (C ₆ H ₆)] <i>anti</i> - μ - η^4 : η^4	arene rotation	12.7	8.1	17.5
	M shift	3.6	1.7	4.8
<i>syn</i> - μ - η^3 : η^3	arene rotation	8.5	9.1	25.7
[[LM] ₂ (C ₆ H ₆)] <i>anti</i> - μ - η^4 : η^4	arene rotation	6.7	5.3	12.0
	M shift	1.4	-0.2 ^[a]	5.2
<i>syn</i> - μ orthogonal	arene rotation	4.1	4.1	4.5 ^[b]

[a] For the parent system, the η^4 : η^2 structure is calculated to be more stable than the η^4 : η^4 structure. Introduction of substituents at N should reverse these stabilities. [b] The η^4 : η^2 structure is more stable than the η^3 : η^3 one.

The most significant difference between the LM and CpM systems is that the deformations away from η^6 coordination (ring slippage, bond localization, ring folding) are consistently more pronounced in the CpM series. This is easily understood from the fragment orbital description of the bonding. The CpM fragment has three valence orbitals and two electrons. So, it tends to bind to an arene using the two empty orbitals, while avoiding repulsion with the third filled one, resulting in strong avoidance of the η^6 structure. In contrast, the LM fragment has two strongly bonding valence orbitals and a third one that is empty but too high in energy for efficient bonding, which results in only a weak avoidance of the η^6 structure.

Conclusion

The complexes described here provide a nice illustration of the influence of steric factors on structural and conformational preferences of arene coordination. For the mononuclear complexes, an η^4 structure is always obtained, with the methyl substitution pattern of the arene directing the preferred orientation. This enabled extraction of “static” NMR parameters for these highly fluxional systems. For the dinuclear complexes, *syn*- μ - η^3 (1,2,3): η^3 (4,5,6) structures would be preferred on electronic grounds, but the bulk of the diiminate ligands forces formation of the *anti*-bridged structures: μ - η^4 (1,2,3,4): η^4 (3,4,5,6) for benzene, toluene and *m*-xylene, and μ - η^3 (1,2,3): η^3 (3,4,5) for mesitylene. Two modes of isomerization (metal shift and ring rotation) were proposed on the basis of calculations. The judicious use of methyl substituents on the arene ring has resulted in a stable analogue of the proposed ring rotation transition state.

Despite the difference in electron count, the structures of diiminate complexes are similar to those of cyclopentadienyl complexes. However, the detailed control over steric factors that is possible with diiminates would be difficult to realize in the cyclopentadienyl series.

Experimental Section

Calculations: All calculations were carried out with the Gaussian-94 program^[5] on SGI workstations. The small split-valence 3-21G basis was used for the first-row atoms.^[6] For Co, Rh, and Ir, relativistic effective core potentials were used for the inner core orbitals and the LanL2DZ basis was used for the valence and outer core electrons;^[7] for Rh and Ir the most diffuse *d* function in that basis was replaced by two components with exponents 1.4142 times higher and lower than the original exponent. Geometries were optimized at the RB3LYP^[8] level within the symmetry constraints mentioned in the Supporting Information (Table S1).

Syntheses: All reactions were carried out under Ar. Solvents were distilled from Na/benzophenone prior to use. [L_{Me}Rh(coe)] and [L_{Cl}Rh(coe)] (coe = cyclooctene) were prepared as reported previously.^[3]

[L_{Me}Rh(benzene)]: L_{Me}Rh(coe) (0.2 g) was dissolved in benzene (10 mL), and the solution was stirred vigorously under a hydrogen atmosphere (1 bar) for 15–45 s. The volatiles were quickly removed in vacuo, and the residue was from that moment on kept below -30 °C (solutions kept at room temperature show virtually complete disproportionation to [[L_{Me}Rh]₂(benzene)] (see below) within 30 min). It was dissolved in [D₈]THF for NMR studies. ¹H NMR (400 MHz, [D₈]THF, -30 °C): δ = 6.96 (d, 4H; *m*), 6.82 (t, 2H; *p*), 4.87 (s, 1H; 3), 4.42 (s, 6H; C₆H₆), 2.28 (s, 12H; *o*-CH₃), 1.37 (s, 6H; 1); ¹³C{¹H} NMR (100.5 MHz, [D₈]THF, -30 °C): δ = 155.5 (2), 154.3 (*i*), 131.5 (*o*), 127.3 (*m*), 123.9 (*p*), 99.3 (3), 96.5 (d, *J*_{Rh,C} (av) = 3.6 Hz; C₆H₆), 21.1 (*l*), 18.2 (*o*-CH₃).

[L_{Me}Rh(C₆H₈)]: [L_{Me}Rh(coe)] (0.2 g) was dissolved in benzene (15 mL) and immediately put under a hydrogen atmosphere (1 bar) and stirred vigorously. An immediate reaction occurs, giving a brown solution. However, completion of the reaction requires prolonged stirring under H₂. After one day, the solvent was removed in vacuo to leave a mixture of [L_{Me}Rh(C₆H₈)] and [[L_{Me}Rh]₂(benzene)] (ca 2:1.3 by NMR spectroscopy) as a red-brown sticky mass (0.19 g). The reaction should not be carried out at higher concentrations of [L_{Me}Rh(coe)], since that leads to even more contamination with [[L_{Me}Rh]₂(C₆H₆)]. ¹H NMR (500.13 MHz, 25 °C, [D₈]THF): δ = 7.07 (br d, 4H; *m*), 6.90 (t, 2H; *p*), 5.09 (s, 1H; 3), 4.26 (m, 2H; cyh 2,3), 2.3 (v br, 12H; *o*-CH₃), 1.66 (s, 6H; 1), 1.64 (m, 2H; cyh 1,4), 1.37 (m, 2H; cyh 5,6 *exo*), 0.54 (m, 2H; cyh 5,6 *endo*); ¹H NMR (-18 °C): δ = 7.13, 7.07 (d, 2H each, *m,m'*), 6.92 (t, 2H; *p*), 5.11 (s, 1H; 3), 4.28 (m, 2H; cyh 2,3), 2.38, 2.16 (s, 6H each, *o,o'*-CH₃), 1.65 (s, 6H; 1), 1.56 (m, 2H; cyh 1,4), 1.37 (m, 2H; cyh 5,6 *exo*), 0.54 (m, 2H; cyh 5,6 *endo*); ¹³C{¹H} NMR (125.76 MHz, -18 °C): δ = 158.9 (2), 157.1 (*i*), 134.0, 131.1 (*o,o'*), 129.6 (*m,m'*), 129.4 (*p*), 99.3 (3), 79.5 (d, *J*_{Rh,C} = 8 Hz; cyh 2,3), 72.4 (d, *J*_{Rh,C} = 12 Hz; cyh 1,4), 24.5, 24.2 (*l*, cyh 5,6), 20.6, 20.2 (*o,o'*-CH₃).

[[L_{Me}Rh]₂(benzene)]: [L_{Me}Rh(coe)] (0.2 g) was dissolved in benzene (2 mL). The solution was heated to 60 °C for 4 h, cooled to room temperature, and the solvent was removed in vacuo. The product was crystallized from hexane. Elemental analysis calcd (%) for C₄₈H₅₆N₂Rh₂ (894.81): C 64.43, H 6.31, N 6.26; found: C 64.25, H 6.37, N 6.10; ¹H NMR (200 MHz, C₆D₁₂, 25 °C): δ = 6.94 (d, 8H; *m*), 6.82 (t, 4H; *p*), 4.86 (s, 2H; 3), 2.14 (s, 24H; *o*-CH₃), 2.12 (s, 6H; C₆H₆), 1.45 (s, 12H; 1); ¹³C{¹H} NMR (50.3 MHz): δ = 156.9 (2), 156.1 (*i*), 132.6 (*o*), 128.8 (*m*), 125.2 (*p*), 99.2 (3), 65.6 (t, *J*_{Rh,C} (av) = 4.8 Hz; C₆H₆), 22.9 (*l*), 19.7 (*o*-CH₃).

[L_{Cl}Rh(benzene)]: This was prepared similarly to [L_{Me}Rh(benzene)], but from [L_{Cl}Rh(coe)]. ¹H NMR (400 MHz, [D₈]THF, -30 °C): δ = 7.35 (d, 4H; *m*), 7.00 (t, 2H; *p*), 4.96 (s, 1H; 3), 4.54 (s, 6H; C₆H₆), 1.48 (s, 6H; 1); ¹³C{¹H} NMR (100.5 MHz): δ = 157.4 (2), 150.6 (*i*), 131.3 (*o*), 127.6 (*m*), 125.3 (*p*), 99.8 (3), 93.2 (d, *J*_{Rh,C} (av) = 5.4 Hz; C₆H₆), 21.2 (*l*).

[L_{Cl}Rh(C₆H₈)]: [L_{Cl}Rh(coe)] (0.2 g) was dissolved in benzene (15 mL) and immediately put in a hydrogen atmosphere (1 bar). The mixture was stirred for one day, and then the solvent was removed in vacuo. The residue was extracted with diethyl ether (5 mL). The extract was concentrated to 0.3 mL and the Schlenk tube was connected to another tube containing hexane (5 mL) to allow slow crystallization by diffusion. A few large brown-red crystals of [L_{Cl}Rh(C₆H₈)] were obtained (0.08 g, 42%). One of these was used for an X-ray structure determination. This reaction, like the synthesis of [L_{Me}Rh(C₆H₈)], should not be carried out at high concentrations. Elemental analysis calcd (%) for C₂₂H₂₁N₂Cl₄Rh (570.15): C 48.45, H 3.71, N 4.91, Cl 24.87; found: C 48.32, H 3.62, N 5.02, Cl 24.71; ¹H NMR (300 MHz, 25 °C, [D₈]THF): δ = 7.45 (d, 4H; *m*), 7.07 (t, 2H; *p*), 5.14 (s, 1H; 3), 4.51 (m, 2H; cyh 2,3), 1.74 (s, 6H; 1), 1.72 (m, 2H; cyh 1,4), 1.46 (m, 2H;

cyh 5,6 *exo*), 0.51 (m, 2H; cyh 5,6 *endo*); $^1\text{H NMR}$ (500.13 MHz, -53°C): $\delta = 7.57, 7.51$ (d, 2H each; *m,m'*), 7.18 (t, 2H; *p*), 5.20 (s, 1H; *3*), 4.53 (m, 2H; cyh 2,3), 1.74 (s, 6H; *I*), 1.57 (m, 2H; cyh 1,4), 1.45 (m, 2H; cyh 5,6 *exo*), 0.52 (m, 2H; cyh 5,6 *endo*); $^{13}\text{C}\{^1\text{H}\}$ (75.4 MHz, 25°C): $\delta = 161.0$ (2), 153.3 (*i*), 133 (br, *o*), 129.8 (*m*), 127.2 (*p*), 99.8 (3), 79.4 (d, $J_{\text{Rh,C}} = 8.3$ Hz; cyh 2,3), 71.4 (d, $J_{\text{Rh,C}} = 12.5$ Hz; cyh 1,4), 24.2 (*I* and cyh 5,6); $^1\text{H NMR}$ (125.76 MHz, -53°C): $\delta = 160.6$ (2), 152.9 (*i*), 134.3, 130.9 (*o,o'*), 130.0 (*m,m'*), 127.7 (*p*), 99.9 (3), 79.0 (cyh 2,3), 71.7 (d, $J_{\text{Rh,C}} = 12$ Hz; cyh 1,4), 24.6, 24.1 (*I*, cyh 5,6).

[$\text{L}_{\text{Me}}\text{Rh}(\text{toluene})$]: This was prepared similarly to [$\text{L}_{\text{Me}}\text{Rh}(\text{benzene})$], but from toluene instead of benzene. $^1\text{H NMR}$ (400 MHz, $[\text{D}_8]\text{THF}$, -30°C): $\delta = 7.05$ (d, 4H; *m*), 6.90 (t, 2H; *p*), 5.65 (t, 1H; tol *p*), 4.91 (s, 1H; *3*), 4.00 (t, 2H; tol *m*), 3.36 (d, 2H; tol *o*), 2.34 (s, 12H; *o-Me*), 1.49 (s, 6H; *I*), 1.23 (s, 3H; tol *Me*); $^{13}\text{C}\{^1\text{H}\}$ (100.5 MHz): $\delta = 157.5$ (2), 156.4 (*i*), 138.4 (tol *i*), 133.6 (*o*), 129.3 (*m*), 125.8 (*p*), 100.9 (3), 99.4 (tol *o*), 85.8 (tol *p*), 82.2 (d, $J_{\text{Rh,C}} = 8$ Hz; tol *m*), 23.1 (*I*), 21.2 (tol *Me*), 20.2 (*o-Me*).

[$\text{L}_{\text{Me}}\text{Rh}_2(\text{toluene})$]: [$\text{L}_{\text{Me}}\text{Rh}(\text{coe})$] (0.2 g) was dissolved in toluene (2 mL). The solution was heated to 60°C for 4 h, cooled to room temperature, and the solvent was removed in vacuo. The product was crystallized from hexane. X-ray quality crystals of [$\text{L}_{\text{Me}}\text{Rh}_2(\text{C}_7\text{H}_8)$] · 3 C_6H_{12} were obtained by recrystallization from cyclohexane. Elemental analysis calcd (%) for $\text{C}_{40}\text{H}_{58}\text{N}_4\text{Rh}_2$ (908.83): C 64.76, H 6.43, N 6.16; found: C 64.97, H 6.44, N 6.32; $^1\text{H NMR}$ (300 MHz; C_6D_{12} , 25°C): $\delta = 6.90$ (d, 8H; *m*), 6.79 (t, 4H; *p*), 4.80 (s, 2H; *3*), 4.21 (t, 1H; tol-*p*), 2.08 (s, 24H; *o-CH}_3*), 1.40 (s, 12H; *I*), 1.34 (s, 3H; tol- CH_3), 1.27 (t, 2H; tol-*m*), 0.57 (d, 2H; tol-*o*); $^{13}\text{C}\{^1\text{H}\}$ NMR (75.4 MHz): $\delta = 157.1$ (2), 156.2 (*i*), 132.7 (*o*), 128.9 (*m*), 125.2 (*p*), 99.1 (3), 88.4 (br. s) and 72.2 (br. s) (tol *i* and *p*), 63.2 (t, $J_{\text{Rh,C}}$ (av) = 6.2 Hz) and 59.9 (t, $J_{\text{Rh,C}}$ (av) = 6.2 Hz) (tol *o* and *m*), 23.0 (*I*), 20.5 (tol- CH_3), 19.8 (*o-CH}_3*).

[$\text{L}_{\text{Me}}\text{Rh}(\text{m-xylene})$]: This was prepared similarly to [$\text{L}_{\text{Me}}\text{Rh}(\text{benzene})$], but with *m*-xylene instead of benzene. $^1\text{H NMR}$ (400 MHz, $[\text{D}_8]\text{THF}$, -30°C): $\delta = 7.06$ (d, 4H; *m*), 6.91 (t, 2H; *p*), 5.22 (d, 2H; xyl 4/6), 4.94 (s, 1H; *3*), 2.32 (s, 12H; *o-Me*), 1.79 (t, 2H; xyl 5), 1.72 (s, 6H; xyl *Me*), 1.50 (s, 6H; *I*), 1.24 (s, 1H; xyl 2); $^{13}\text{C}\{^1\text{H}\}$ NMR (100.5 MHz): $\delta = 157.7$ (2), 156.4 (*i*), 133.6 (*o*), 129.3 (*m*), 125.8 (*p*), 122.5 (xyl 1/3), 104.2 (xyl 4/6), 101.0 (3), 76.0 (d, $J = 8$ Hz; xyl 3), 75.0 (d, $J_{\text{Rh,C}} = 10$ Hz; xyl 5), 23.3 (*I*), 21.9 (xyl *Me*), 20.3 (*o-Me*).

[$\text{L}_{\text{Me}}\text{Rh}_2(\text{m-xylene})$]: Crude [$\text{L}_{\text{Me}}\text{Rh}(\text{m-xylene})$] (as described above) (0.2 g) was dissolved in THF (3 mL). After this solution had been left to stand for one day at room temperature, the volatiles were removed in vacuo, and the residue was crystallized from pentane (RT to -20°C), to give brown [$\text{L}_{\text{Me}}\text{Rh}_2(\text{m-xylene})$] (0.11 g; 61%). Elemental analysis calcd (%) for $\text{C}_{50}\text{H}_{60}\text{N}_4\text{Rh}_2$ (922.86): C 65.07, H 6.55, N 6.07; found: C 64.95, H 6.67, N 6.06; $^1\text{H NMR}$ (400 MHz, $[\text{D}_8]\text{THF}$, 25°C): $\delta = 7.02$ (d, 8H; *m*), 6.88 (t, 4H; *p*), 4.87 (s, 2H; *3*), 2.72 (t, 1H; xyl 5), 2.35 (d, 2H; xyl 4/6), 2.14 (s, 24H; *o-CH}_3*), 1.39 (s, 12H; *I*), 0.23 (s, 6H; xyl *Me*), 0.12 (br. s, 1H; xyl 2); $^{13}\text{C}\{^1\text{H}\}$ NMR (100.5 MHz): $\delta = 157.7$ (2), 156.4 (*i*), 133.5 (*o*), 130.0 (*m*), 126.1 (*p*), 99.5 (3), 89.1 (t, $J = 4$ Hz; xyl 1/3), 67.3 (br. s; xyl 2), 62.3 (t, $J = 5$ Hz; xyl 4/6), 59.0 (t, $J = 7$ Hz; xyl 5), 23.7 (*I*), 20.5 (xyl *Me*), 20.4 (*o-CH}_3*).

[$\text{L}_{\text{Me}}\text{Rh}(\text{mesitylene})$]: This was prepared similarly to [$\text{L}_{\text{Me}}\text{Rh}(\text{benzene})$], but disproportionates more slowly, particularly in alkanes. $^1\text{H NMR}$ (200 MHz, C_6D_{12} , 25°C): $\delta = 7.15$ (d, 4H; *m*), 6.99 (t, 2H; *p*), 5.06 (s, 1H; *3*), 3.88 (s, 3H; $\text{Me}_3\text{C}_6\text{H}_3$), 2.55 (s, 12H; *o-CH}_3*), 1.55 (s, 6H; *I*), 1.18 (s, 9H; $\text{Me}_3\text{C}_6\text{H}_3$); $^{13}\text{C}\{^1\text{H}\}$ (50.4 MHz): $\delta = 156.1$ (2), 154.3 (*i*), 133.6 (*o*), 128.9 (*m*), 124.6 (*p*), 116.0 (d, $J_{\text{Rh,C}}$ (av) = 4.6 Hz; *mes I*), 101.4 (3), 95.8 (d, $J_{\text{Rh,C}}$ (av) = 4.1 Hz; *mes 2*), 22.5 (*I*), 21.3 ($\text{Me}_3\text{C}_6\text{H}_3$), 19.3 (*o-CH}_3*).

[$\text{L}_{\text{Me}}\text{Rh}_2(\text{mesitylene})$]: Crude [$\text{L}_{\text{Me}}\text{Rh}(\text{mesitylene})$] (as described above) (0.2 g) was dissolved in pentane (3 mL). Over a period of days, nearly black [$\text{L}_{\text{Me}}\text{Rh}_2(\text{mesitylene})$] was deposited (0.13 g, 73%). Crystals suitable for X-ray studies were obtained by carrying out the disproportionation in THF. Elemental analysis calcd (%) for $\text{C}_{51}\text{H}_{62}\text{N}_4\text{Rh}_2$ (936.89): C 65.38, H 6.67, N 5.98; found: C 65.41, H 6.66, N 6.10; $^1\text{H NMR}$ (400 MHz, $[\text{D}_8]\text{THF}$, 25°C): $\delta = 7.03$ (d, 8H; *m*), 6.89 (t, 4H; *p*), 4.81 (s, 2H; *3*), 2.17 (s, 24H; *o-CH}_3*), 1.35 (s, 12H; *I*), 0.90 (s, 3H; *mes 2/4/6*), 0.42 (s, 9H; xyl *Me*); $^{13}\text{C}\{^1\text{H}\}$ (100.5 MHz): $\delta = 157.1$ (2), 155.3 (*i*), 133.8 (*o*), 130.3 (*m*), 126.0 (*p*), 103.1 (*mes 1/3/5*), 99.2 (3), 58.1 (*mes 2/4/6*), 23.5 (*I* and *mes Me*), 20.2 (*o-CH}_3*).

Crystal structure determinations: Crystals were mounted in thin-walled glass capillaries under Ar. Details of all structure determinations are collected in Table 5. Since the glass capillaries prevented accurate description of the crystal shape, semi-empirical absorption corrections^[9] were applied; for [$\text{L}_{\text{Me}}\text{Rh}_2(\text{mesitylene})$], this proved to be insufficient and

the DIFABS procedure^[20] was used to improve the empirical absorption correction. Structures were solved with the PATTY option^[21] of the DIRDIF program system.^[22] Refinements were carried out with the SHELXL-97 package.^[23] All non-hydrogen atoms were refined with anisotropic temperature factors. The hydrogen atoms were placed at calculated positions and refined isotropically in riding mode. The positions of the vinylic hydrogen atoms of [$\text{L}_{\text{C}_1}\text{Rh}(\text{cyclohexadiene})$] and the toluene hydrogen atoms of [$\text{L}_{\text{Me}}\text{Rh}_2(\text{toluene})$] · 3 C_6H_{12} were subsequently refined independently. The solvent cyclohexane molecules of [$\text{L}_{\text{Me}}\text{Rh}_2(\text{toluene})$] · 3 C_6H_{12} were slightly disordered, resulting in fairly large anisotropic average displacement parameters. Efforts to fit the observed electron density with partially occupied disordered molecules did not result in physically reasonable models. All refinements were full-matrix least-squares on F^2 . Geometrical calculations^[24] revealed neither unusual geometric features, nor unusual short intermolecular contacts, and the calculations revealed no higher symmetry and no solvent accessible areas. Crystallographic data (excluding structure factors) for the structures reported in this paper have been deposited with the Cambridge Crystallographic Data Centre as supplementary publication nos. CCDC-103103, CCDC-103102, and CCDC-138287. Copies of the data can be obtained free of charge on application to CCDC, 12 Union Road, Cambridge CB2 1EZ, UK (fax: (+44) 1223 336-033; e-mail: deposit@ccdc.cam.ac.uk).

Acknowledgement

We thank Mr P. P. J. Schlebos for his able assistance with numerous NMR measurements, the Dutch Polymer Institute for providing most of the funds to purchase our computing equipment and software, and Johnson Matthey for a generous loan of rhodium chloride.

- [1] For a review of bridging arene complexes, see H. Wade, *Angew. Chem.* **1992**, *104*, 253; *Angew. Chem. Int. Ed. Engl.* **1992**, *31*, 247.
- [2] J. W. Lauher, M. Elian, R. H. Summerville, R. Hoffmann, *J. Am. Chem. Soc.* **1976**, *98*, 3219.
- [3] P. H. M. Budzelaar, N. N. P. Moonen, R. de Gelder, J. M. M. Smits, A. W. Gal, *Eur. J. Inorg. Chem.* **2000**, 753; P. H. M. Budzelaar, R. de Gelder, A. W. Gal, *Organometallics* **1998**, *17*, 4122.
- [4] J. J. Schneider, U. Denninger, O. Heinemann, C. Krüger, *Angew. Chem.* **1995**, *107*, 631; *Angew. Chem. Int. Ed. Engl.* **1995**, *34*, 592; J. J. Schneider, D. Wolf, C. Janiak, O. Heinemann, J. Rust, C. Krüger, *Chem. Eur. J.* **1998**, *4*, 1982.
- [5] Oxidative addition of aromatic C–halide bonds will be described separately.
- [6] Various η^2 , η^3 , and η^6 models produced much poorer fits, with average deviations of 8–10 ppm in the predicted ^{13}C shifts.
- [7] $\text{L}_2 = \text{dppe}$: M. J. Nolte, G. Gafner, *Acta Crystallogr.* **1974**, *B30*, 738; $\text{L} = \text{P}(\text{OMe})_3$: P. Albano, M. Areats, M. Manassero, *Inorg. Chem.* **1980**, *19*, 1069. In both complexes, the coordinated arene shows a clear boat distortion, but the structures are still clearly η^6 .
- [8] In contrast to the $\eta^4:\eta^4$ structure, one cannot write a valence-bond structure for the $\eta^3:\eta^3$ structure without charge separation. In MO terms, however, the bonding in the two complexes is very similar: the LRh fragments each overlap with one of the orthogonal arene π HOMOs, and the difference between $\eta^4:\eta^4$ and $\eta^3:\eta^3$ just corresponds to a different choice of the HOMO nodal planes. Drawing a charge-separated valence bond structure for $\eta^3:\eta^3$ but not for $\eta^4:\eta^4$ would therefore be misleading.
- [9] Calculated Rh–C(arene) distances are consistently too large by 0.1–0.2 Å. Apparently, the method employed here systematically underestimates olefin and arene coordination to Rh^I. Similar deviations were found in previous work.^[3]
- [10] J. Müller, P. Escarpa Gaede, K. Qiao, *Angew. Chem.* **1993**, *105*, 1809; *Angew. Chem. Int. Ed. Engl.* **1993**, *32*, 1697.
- [11] J. Müller, K. Ha, O. Lettau, R. Schubert, *Z. Anorg. Allg. Chem.* **1998**, *624*, 192.
- [12] J. J. Schneider, U. Specht, R. Goddard, C. Krüger, J. Ensling, P. Güthlich, *Chem. Ber.* **1995**, *128*, 941.
- [13] A. J. Blake, P. J. Dyson, B. F. G. Johnson, C. M. Martin, *J. Chem. Soc. Chem. Commun.* **1994**, 1471.

Table 5. Details of X-ray structure determinations.

	[L _{Cl} Rh(cyclohexadiene)]	[(L _{Me} Rh) ₂ (toluene)] · 3 C ₆ H ₁₂	[L _{Me} Rh] ₂ (mesitylene)
crystal color	transparent red-brown	black	black
crystal shape	rather regular fragment	rather regular fragment	rough fragment
crystal size [mm]	0.70 × 0.38 × 0.28	0.44 × 0.31 × 0.19	0.70 × 0.36 × 0.28
empirical formula	C ₂₃ H ₂₁ Cl ₄ N ₂ Rh	C ₆₇ H ₆₄ N ₄ Rh ₂	C ₅₁ H ₆₂ N ₄ Rh ₂
formula weight	570.13	1161.28	936.87
temperature [K]	293(2)	208(2)	208(2)
radiation (graphite monochromated)	Cu _{Kα}	Cu _{Kα}	Mo _{Kα}
wavelength [Å]	1.54184	1.54184	0.71073
crystal system	orthorhombic	triclinic	monoclinic
space group	<i>Pbca</i>	<i>P</i> $\bar{1}$	Cc
unit cell: no of reflections	25	25	24
θ range (°)	40.131 to 46.470	40.342 to 46.309	19.266 to 23.034
<i>a</i> [Å]	9.2719(6)	12.5889(13)	15.538(5)
<i>b</i> [Å]	17.7995(6)	14.3317(16)	23.070(10)
<i>c</i> [Å]	27.7423(11)	18.2523(16)	14.521(3)
α [°]	90	72.243(8)	90
β [°]	90	84.139(8)	120.90(2)
γ [°]	90	81.696(9)	90
volume [Å ³]	4578.5(4)	3097.4(5)	4466(3)
<i>Z</i> , calc. density [Mgm ⁻³]	8, 1.654	2, 1.245	4, 1.393
abs. coefficient [mm ⁻¹]	10.429	4.609	0.778
diffractometer	Enraf-Nonius CAD4	Enraf-Nonius CAD4	Enraf-Nonius CAD4
scan	$\theta/2\theta$	$\theta/2\theta$	ω
<i>F</i> (000)	2288	1228	1944
θ range for data collection (°)	3.19 to 69.89	3.26 to 59.96	2.89 to 27.45
index ranges	0 ≤ <i>h</i> ≤ 11 0 ≤ <i>k</i> ≤ 21 0 ≤ <i>l</i> ≤ 33	−14 ≤ <i>h</i> ≤ 13 −16 ≤ <i>k</i> ≤ 0 −20 ≤ <i>l</i> ≤ 19	−20 ≤ <i>h</i> ≤ 0 0 ≤ <i>k</i> ≤ 29 −16 ≤ <i>l</i> ≤ 18
refl. collected/unique	4333/4333	9594/9168	5271/5271
[<i>R</i> _{int}]		[0.0690]	
refl. observed [<i>I</i> _o > 2σ(<i>I</i> _o)]	2458	4990	4167
abs. corr.	semiempirical ψ scan	semiempirical ψ scan	semiempirical ψ scan + DIFABS
ψ scan transm. factors	1.330 to 0.835	1.227 to 0.855	1.064 to 0.962
DIFABS corr. factors			0.881 to 1.114
data/restraints/parameters	4333/0/285	9168/0/686	5271/2/529
goodness-of-fit on <i>F</i> ²	1.057	1.041	1.046
SHELXL-97 wt parameters	0.0844, 10.8361	0.0456 9.922	0.0316, 2.3141
final <i>R</i> ₁ , <i>wR</i> ₂ [<i>I</i> > 2σ(<i>I</i>)]	0.0513, 0.1333	0.0656, 0.1226	0.0262, 0.0560
<i>R</i> ₁ , <i>wR</i> ₂ (all data)	0.0643, 0.1429	0.1509, 0.1539	0.0455, 0.0626
diff. peak and hole [e Å ⁻³]	2.463 and −1.432	0.714 and −1.239	0.342 and −0.3530

- [14] For a recent theoretical study covering mononuclear [CpCo(benzene)], see J. H. Hardesty, J. B. Koerner, T. A. Albright, G.-Y. Lee, *J. Am. Chem. Soc.* **1999**, *121*, 6055.
- [15] M. J. Frisch, G. W. Trucks, H. B. Schlegel, P. M. W. Gill, B. G. Johnson, M. A. Robb, J. R. Cheeseman, T. Keith, G. A. Petersson, J. A. Montgomery, K. Raghavachari, M. A. Al-Laham, V. G. Zakrzewski, J. V. Ortiz, J. B. Foresman, J. Cioslowski, B. B. Stefanov, A. Nanayakkara, M. Challacombe, C. Y. Peng, P. Y. Ayala, W. Chen, M. W. Wong, J. L. Andres, E. S. Replogle, R. Gomperts, R. L. Martin, D. J. Fox, J. S. Binkley, D. J. Defrees, J. Baker, J. P. Stewart, M. Head-Gordon, C. Gonzalez, J. A. Pople, *Gaussian 94, Revision E.1*, Gaussian Inc., Pittsburgh PA, **1995**.
- [16] S. Binkley, J. A. Pople, W. J. Hehre, *J. Am. Chem. Soc.* **1980**, *102*, 939.
- [17] P. J. Hay, W. R. Wadt, *J. Chem. Phys.* **1985**, *82*, 299.
- [18] A. D. Becke, *J. Chem. Phys.* **1993**, *98*, 5648.
- [19] A. C. T. North, D. C. Philips, F. S. Mathews, *Acta Crystallogr. Sect. A* **1968**, *24*, 351.
- [20] N. Walker, D. Stuart, *Acta Crystallogr. Sect. A* **1983**, *39*, 158.
- [21] P. T. Beurskens, G. Beurskens, M. Strumpel, C. E. Nordman in *Patterson and Pattersons* (Eds.: J. P. Glusker, B. K. Patterson, M. Rossi), Clarendon, Oxford, **1987**, p. 356.
- [22] P. T. Beurskens, G. Beurskens, W. P. Bosman, R. de Gelder, S. Garcia-Granda, R. O. Gould, R. Israel, J. M. M. Smits, DIRDIF-96. A computer program system for crystal structure determination by Patterson methods and direct methods applied to difference structure factors, Crystallography Laboratory, University of Nijmegen, The Netherlands, **1996**.
- [23] G. M. Sheldrick, SHELXL-97. Program for the refinement of crystal structures, University of Gottingen: Germany, **1997**.
- [24] A. L. Spek, *Acta Crystallogr. Sect. A* **1990**, *46*, C-34; A. L. Spek, PLATON-93. Program for display and analysis of crystal and molecular structures, University of Utrecht, The Netherlands, **1995**.

Received: December 29, 1999 [F2217]